Structure and Mechanism of Action of an Inverting Mutant Sialidase†

Simon Newstead,‡ Jacqueline N. Watson,§ Tara L. Knoll,§ Andrew J. Bennet,*,§ and Garry Taylor*,‡

Centre for Biomolecular Science, University of St. Andrews, St. Andrews, Fife KY16 9ST, Scotland, and Department of Chemistry, Simon Fraser University, 8888 University Drive, Burnaby, British Columbia V5A 1S6, Canada

Received March 21, 2005; Revised Manuscript Received April 30, 2005

ABSTRACT: Mutagenesis of the conserved tyrosine (Y370) of the *Micromonospora viridifaciens* sialidase to small amino acids changes the mechanism of catalysis from retention of anomeric configuration to inversion [Watson, J. N., et al. (2003) *Biochemistry 42*, 12682−12690]. For the Y370G mutant enzyme-catalyzed hydrolysis of a series of aryl sialosides and 3′-sialyllactose, the derived Brønsted parameters (β_{lg}) on k_{cat} and k_{cat}/K_m are -0.63 ± 0.05 and -0.80 ± 0.08, respectively. Thus, for the Y370G enzyme, glycosidic C−O bond cleavage is rate-determining. Analysis of the activity of the Y370G mutant and wild-type enzymes against a substrate [3,4-dihydro-2*H*-pyrano[3,2-*c*]pyridinium α-D-*N*-acetylneuraminide (DHP-αNeu5Ac)] whose hydrolysis cannot be accelerated by acid catalysis is consistent with these reactions proceeding via S_N1 and S_N2 mechanisms, respectively. The overall structure of the Y370G mutant sialidase active site is very similar to the previously reported wild-type structure [Gaskell, A., et al. (1995) *Structure 3*, 1197−1205], although removal of the tyrosine residue creates two significant changes to the active site. First, the anomeric oxygen atom of the hydrolysis product (β-*N*-acetylneuraminic acid) and four water molecules bind in the large cavity created by the Y370G mutation. Second, the side chain of Asn310 moves to make a strong hydrogen bond to one of the bound water molecules.

The enzymes that cleave the terminal sialic acid residues, which are α-ketosidically linked to glycoconjugates, are exo-sialidases (*N*-acetylneuraminosyl glycohydrolase, neuraminidase, EC 3.2.1.18) (*1*). These enzymes are involved in the pathogenesis of many human diseases, including influenza and cholera (*2*, *3*). Within the exo-sialidase superfamily, sequence homology and X-ray crystal structure data have revealed that seven amino acid residues are strictly conserved (*4*). Three of these seven residues, a conserved tyrosine and a pair of acidic residues (glutamic and aspartic acid), are thought to comprise the basic catalytic assembly (*4*). A salient feature of all known exo-sialidases is that catalysis occurs with retention of the anomeric configuration (*5*−*7*).

Recently, Withers and co-workers have shown that the acid−base catalyst mutant (D59A) *trans*-sialidase from *Trypanosoma cruzi* becomes covalently modified on the active site tyrosine residue during the slow turnover of 3-fluoro-α-D-*N*-acetylneuraminosyl fluoride (*8*, *9*), a finding consistent with a tyrosine residue being the catalytic nucleophile. A similar conclusion was reached by Watson et al. (*10*), who reported that three tyrosine mutants of the *Micromonospora viridifaciens* sialidase (Y370A, Y370D, and Y370G) were catalytically active inverting enzymes. In other words, replacement of the nucleophilic tyrosine residue with a smaller amino acid changes the mechanism of hydrolysis from one involving two inversions of configuration via a tyrosinyl-bound intermediate to one in which a bound water molecule gives rise to a direct displacement reaction that entails a single inversion of configuration. On the basis of structural (*11*), kinetic (*12*), and computational (*13*) studies, it has been proposed that the conserved aspartic acid residue acts as a general acid catalyst. Furthermore, Watson et al. (*14*) concluded that the contribution of this residue to catalysis is much more important for the hydrolysis of natural substrates than for the corresponding reactions of aryl *N*-acetylneuraminides.

It is perhaps surprising that *M. viridifaciens* Y370 mutant sialidases possess close to wild-type activity against moderately activated substrates, but it is possible that for good leaving groups the conserved glutamic acid residue can assist the nucleophilic attack of the bound water molecule via a general base-catalyzed process. In contrast, nucleophilic mutants of acetal-processing glycosidases display a much greater reduction in their catalytic activity when water is the nucleophile. For example, Wang et al. noted that the E358A mutant β-glucosidase from *Agrobacterium* displayed a k_{cat} value that is reduced by a factor of greater than 10^7 in comparison to that of the wild-type enzyme for the hydrolysis of the activated substrate 2,4-dinitrophenyl glucoside (*15*). Moreover, Wang et al. noted that the activity of their nucleophilic mutant could be rescued by the addition of strong, small anionic nucleophiles such as formate and azide (*15*), and similar observations have been reported for other mutant acetal-processing glycosidases (*16*−*19*).

† This work was supported by the Natural Sciences and Engineering Research Council of Canada. S.N. gratefully acknowledges a UK Biology and Biotechnology Science Research Council studentship.

* To whom correspondence should be addressed. A.J.B.: e-mail, bennet@sfu.ca; telephone, (604) 291-4884; fax, (604) 291-5424. G.T.: e-mail, glt2@st-and.ac.uk; telephone, +44-(0)1334-467301; fax, +44-(0)1334-462595.

‡ University of St. Andrews.

§ Simon Fraser University.

10.1021/bi050517t CCC: $30.25
Published on Web 06/01/2005

Table 1: Summary of Crystallographic Information

resolution range (Å)	105−1.8
no. of observations	117043
R_{merge} (%)[a]	9.0 (21.5)
$I/\sigma(I)$	5.0 (3.0)
no. of unique reflections	46213
completeness (%)	87.3 (87.3)
R (%)[b]	14.1
R_{free} (%)	20.1
rmsd for bond lengths (Å)	0.02
rmsd for bond angles (deg)	1.79
su of atom positions[c] (Å)	0.103 ± 0.028
no. of protein atoms and solvent atoms	4548 and 849
average B values for protein atoms (Å^2)	15.0
average B values for β-Neu5Ac (Å^2)	10.7
PDB entry	2BER

[a] $R_{merge} = \sum|I(k) - \langle I\rangle|/\sum I(k)$, where $I(k)$ is the value of the kth measurement of the intensity of a reflection, $\langle I\rangle$ is the mean value of the intensity of that reflection, and the summation is over all measurements. Values in parentheses are for the highest-resolution shell. [b] $R = \sum_{hkl}|F_{obs} - F_{calc}|/\sum_{hkl}|F_{obs}|$. R_{free} is calculated in the same way as the R, but for a 5% test set excluded from the refinement. [c] The standard radial uncertainty of an atom with the average B factor was estimated using the DPI (diffraction precision indicator) method proposed by Cruickshank (*34*) as implemented in ESCET (*35*).

This paper details a complementary series of kinetic and structural studies that were performed on the Y370G mutant of the sialidase from *M. viridifaciens* using a variety of substituted aryl α-D-*N*-acetylneuraminides (**1**), a natural substrate analogue (3′-sialyllactose, **2**), and a pyridinium α-D-*N*-acetylneuraminide (**3**).

EXPERIMENTAL PROCEDURES

Materials. All chemicals were of analytical grade or better. MU-αNeu5Ac,[1] PNP-αNeu5Ac, and phenyl α-D-*N*-acetylneuraminide were purchased from Sigma-Aldrich, and 3′-SL was purchased from V-labs. DHP-αNeu5Ac (*20*) and DANA (*21*, *22*) were synthesized according to literature procedures.

Enzyme Kinetics. The enzyme-catalyzed hydrolysis reactions of DHP-αNeu5Ac were monitored by following the decrease in absorbance at 266 nm ($\Delta\epsilon = -6221$ M^{-1} cm^{-1}) using a Cary 3E UV−vis spectrophotometer equipped with the Cary six-cell Peltier constant-temperature accessory. Kinetic data for all other substrates were acquired using protocols identical to those reported earlier (*10*). Michaelis−Menten parameters were calculated using a standard nonlinear least-squares fit of the rate versus substrate concentration data. To measure the binding affinity of DANA for Y370G, the rate of hydrolysis of MU-αNeuAc at a concentration well below K_m was monitored in the presence of varying DANA concentrations. To obtain a value for K_i, the kinetic data were fit to the standard equation for competitive inhibition (using GraFit). To determine whether the Y370G mutant can hydrate DANA, NMR experiments were performed using 10 mM DANA in tartrate buffer (10 mM in D_2O at pD 5.3) at room temperature. The concentration of the enzyme in the reaction was one-tenth of that used to determine the stereochemical outcome of MUαNeuAc hydrolysis (*10*). The DANA-containing reaction was monitored for 20 h.

Protein Crystallization. The purified protein was concentrated to 20 mg/mL in 20 mM sodium phosphate (pH 7.0) and crystallized using the sitting drop vapor diffusion method. Crystals appeared within 1−2 weeks at 293 K in drops composed of 2 μL of protein solution and 2 μL of mother liquor containing 13% (w/w) PEG 3350 and 0.2 M sodium fluoride. The crystals were soaked in situ with 40 mM DHP-αNeu5Ac for 30 min at 293 K. Crystals were cryoprotected in 20% (w/v) glycerol in the crystallization buffer for 1 min prior to being flash-frozen in a nitrogen stream at 100 K.

X-ray Data Collection. Diffraction data were collected to 1.8 Å on a MAR CCD 3×3 detector on beamline ID14.3 at the European Synchrotron Radiation Facility (ESRF). The diffraction images were processed using MOSFLM (*23*) and scaled and merged using SCALA (*24*) from the CCP4 package (*25*). The data processing statistics are summarized in Table 1. The crystal belongs to space group $P2_1$, with the following unit cell dimensions: $a = 55.44$ Å, $b = 49.54$ Å, $c = 107.04$ Å, and $\beta = 101.74°$. The crystal has a solvent content of 41.4% with one molecule in the asymmetric unit and a Mathews coefficient of 2.1 Å^3 Da^{-1}.

Structure Determination. The starting model for crystallographic refinement was the 1.6 Å structure of the *M. viridifaciens* D92G mutant sialidase reported previously (*14*), PDB entry 1W8N, which was in an orthorhombic $P2_12_12_1$ unit cell. A molecular replacement solution in the new monoclinic cell was found using the complete model with AMoRE (*26*). Rigid body refinement of the three domains (residues 47−402, 403−502, and 503−647) was followed by restrained refinement using REFMAC5 (*27*), with iterative cycles of model building in O (*28*). Solvent molecules were added automatically using ARP/wARP (*29*) and visually inspected for correct placement in O (*28*). The final crystallographic statistics are summarized in Table 1. Atomic coordinates have been deposited in the Protein Data Bank as entry 2BER.

RESULTS

Enzyme Kinetics. Given in Table 2 are the kinetic parameters for the Y370G mutant *M. viridifaciens* sialidase-catalyzed hydrolysis of a panel of substrates (**1**−**3**). Included

Table 2: Michaelis−Menten Kinetic Parameters for the Y370G Mutant Sialidase Measured at pH 5.25 and 37 °C

aglycon (lg)	pK_a (lg−H$^+$)[a]	substrate	k_{cat}[a] (s^{-1})	k_{cat}/K_m[b] (M^{-1} s^{-1})	K_d (M)
4-nitrophenol	7.18	**1a**	123 ± 6	(1.1 ± 0.3) × 10^6	(1.1 ± 0.2) × 10^{-4}
4-MU[c]	7.80	**1b**	44.3 ± 0.1	(1.3 ± 0.2) × 10^6	(3.5 ± 0.6) × 10^{-5}
phenol	9.92	**1c**	0.82 ± 0.04	(3.6 ± 0.7) × 10^4	(2.3 ± 0.3) × 10^{-5}
3′-lactose	13.6[b]	**2**	1.2 × 10^{-2} [d]	12.6	(9.5 ± 2.6) × 10^{-4}
DHP	7.18[e]	**3**	<2 × 10^{-4} [f]	<1.8[f]	(5.0 ± 0.6) × 10^{-5} [g]

[a] Data taken from ref *36*. [b] Estimated value taken from ref *10*. [c] Data taken from ref *10*. [d] No error is associated with these values because they are estimates based on a single rate measurement at a high concentration of substrate and enzyme. [e] Data taken from ref *20*. [f] Upper limit. [g] Calculated according to ref *37*. $IC_{50} = (1.6 \pm 0.2) \times 10^{-4}$ (see Experimental Procedures for full details).

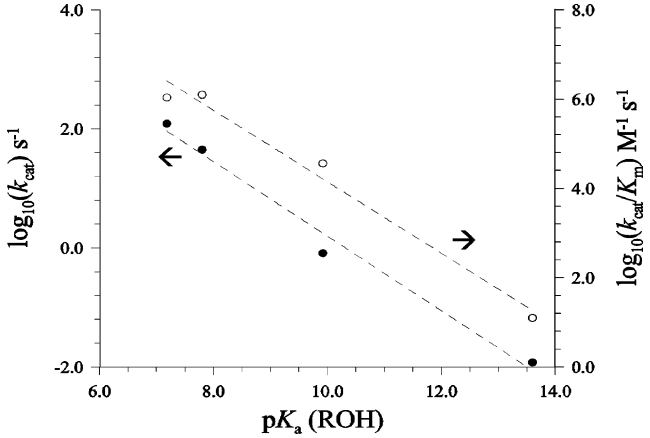

FIGURE 1: Brønsted plots. Effect of leaving group ability on k_{cat} (●) and k_{cat}/K_m (○) for the Y370G mutant sialidase at 37 °C and pH 5.25. The leaving group ability is represented as pK_a(BH^+) as follows: 7.18 for 4-nitrophenol, 7.80 for 4-methylumbelliferone, 9.92 for phenol, and ~13.6 for lactose (3′-OH).

in this panel of substrates are (a) aryl α-sialosides (**1a**−**c**), (b) a natural substrate analogue, α-D-sialosyl(2→3)lactose (**2**), and (c) a pyridinium α-sialoside (**3**).

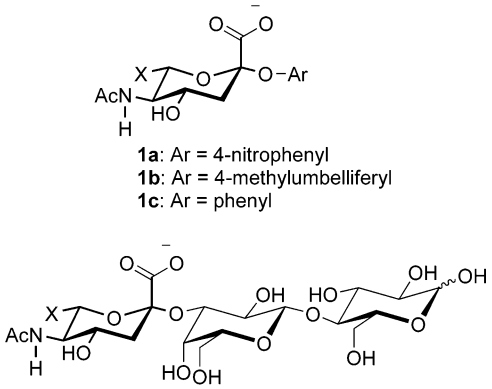

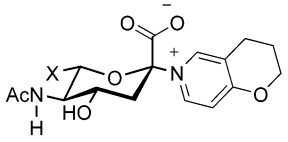

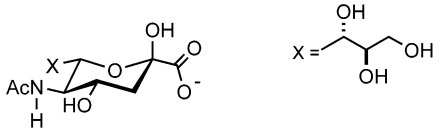

Figure 1 shows the Brønsted plots for the Y370G mutant-catalyzed hydrolyses of substrates that contain the natural C−O glycosidic linkage. The derived β_{lg} values on kinetic parameters k_{cat} and k_{cat}/K_m are −0.63 ± 0.05 and −0.80 ± 0.08, respectively.

[1] Abbreviations: DANA, 2-deoxy-2,3-didehydro-*N*-acetylneuraminic acid; DHP-αNeu5Ac, 3,4-dihydro-2*H*-pyrano[3,2-*c*]pyridinium α-D-*N*-acetylneuraminide; MU-αNeu5Ac, 4-methylumbelliferyl α-D-*N*-acetylneuraminide; MvNA, *M. viridifaciens* neuraminidase; Neu5Ac, *N*-acetylneuraminic acid; PNP-αNeu5Ac, *p*-nitrophenyl α-D-*N*-acetylneuraminide; 3′-SL, α-D-sialosyl(2→3)lactose; rmsd, root-mean-square deviation.

Table 3: Catalytic Proficiencies (CP) for the Wild-Type Recombinant *M. viridifaciens* Sialidase and Y370G and D92G Variants with PNP-αNeu5Ac and DHP-αNeu5Ac at pH 5.25 and 37 °C

sialidase	PNP-αNeu5Ac CP (M^{-1})[a]	DHP-αNeu5Ac CP (M^{-1})[b]
wild-type	1.7×10^{12} [c]	2.2×10^{11} [d]
Y370G	2.2×10^{11}	$<4 \times 10^{7}$
D92G	1.1×10^{12} [e]	1.1×10^{12} [f]

[a] The extrapolated value of k_{uncat} for PNP-αNeu5Ac at 37 °C is 5.0×10^{-6} s^{-1} (*38*). [b] The extrapolated value of k_{uncat} for DHP-αNeu5Ac at 37 °C is 8.6×10^{-8} s^{-1} (*20*). [c] Data taken from ref *10*. [d] Measured values for k_{cat} and k_{cat}/K_m are 0.127 ± 0.007 s^{-1} and (1.92 ± 0.46) × 10^4 M^{-1} s^{-1}, respectively. [e] Data taken from ref *14*. [f] Measured values for k_{cat} and k_{cat}/K_m are 0.300 ± 0.008 s^{-1} and (1.00 ± 0.18) × 10^5 M^{-1} s^{-1}, respectively.

Table 3 lists the catalytic proficiency of both the wild-type and Y370G mutant *M. viridifaciens* sialidases for the hydrolysis of PNP-αNeu5Ac (**1a**) and DHP-αNeu5Ac (**3**). Catalytic proficiency (CP) is defined as the ratio of two rate constants, the second-order rate constant for the enzyme-catalyzed hydrolysis of the substrate (k_{cat}/K_m) and the pseudo-first-order rate constant (k_{uncat}) for the uncatalyzed reaction (eq 1).

$$CP = (k_{cat}/K_m)/k_{uncat}\ (M^{-1}) \quad (1)$$

To determine whether these catalyzed reactions give DANA as either a product or an intermediate, the Y370G mutant was incubated in the presence of DANA for 20 h. Under these conditions, no formation of *N*-acetylneuraminic acid was observed, yet DANA binds to this enzyme with a K_i value of (5.5 ± 1.8) × 10^{-6} M. Assuming that 10% hydration would have been detected, the maximal value for k_{cat} for hydration of DANA by Y370G is 0.09 s^{-1}. In addition, during the Y370G mutant-catalyzed hydrolysis of PNP-αNeu5Ac (**1a**), the only reaction product formed is *N*-acetylneuraminic acid (data not shown); that is, no evidence was seen for the formation of DANA. Thus, it can be concluded that the Y370G mutant catalyzes a substitution reaction and not an elimination reaction.

Structural Studies. In 2003, Watson et al. (*10*) noted that mutation of the conserved catalytic tyrosine residue to a smaller amino acid (A, D, or G) resulted in a change in the mechanism from retention to inversion of configuration. The authors proposed that the mutation created a "hole" in the active site from which a bound water molecule could effectively function as the catalytic nucleophile. To investigate the structural consequences of such nonconservative mutations, the Y370G mutant described in the 2003 paper was crystallized and soaked with DHP-αNeu5Ac (as described in Experimental Procedures). The result of this experiment revealed unambiguous density for β-Neu5Ac (**4**) sitting in the active site (Figure 2). Clearly, DHP-αNeu5Ac either was turned over slowly by the Y370G mutant or underwent partial spontaneous hydrolysis during the soaking experiment to give some Neu5Ac, which forms a mixed population of the α- and β-anomers in solution.

The overall structure of the Y370G active site is very similar to the previously reported wild-type structure (PDB entry 1EUS) (*30*), with an rmsd of only 0.36 Å for the 359 equivalent C_α atoms that make up the β-propeller catalytic domain. However, removal of the tyrosine residue creates

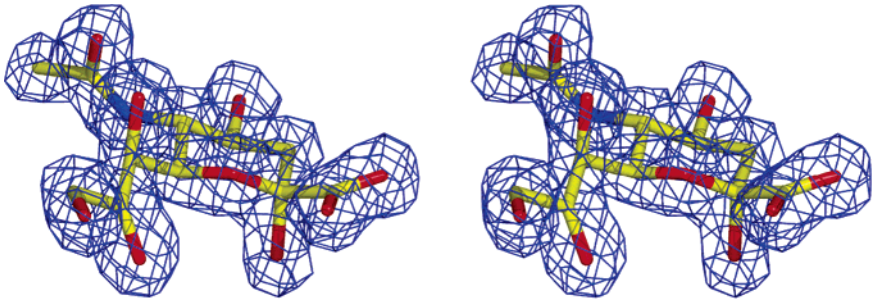

FIGURE 2: Stereoview showing the refined maximum-likelihood σ_A weighted $2F_o - F_c$ electron density map for the β-Neu5Ac ligand, contoured at 2σ.

Table 4: Hydrogen Bonding Interactions between the Bound Ligand, β-Neu5Ac, and the Active Site of the Y370G MvNA Mutant

β-Neu5Ac	protein or water atom	distance (Å)
O1A	Arg276 $N^{\eta 1}$	3.20
	Arg276 $N^{\eta 2}$	2.99
	Arg342 $N^{\eta 2}$	2.94
	H_2O	3.11
O1B	Arg342 $N^{\eta 1}$	3.07
	Arg68 $N^{\eta 1}$	2.98
	Arg266 $N^{\eta 2}$	3.02
O2	Arg276 $N^{\eta 1}$	3.05
	H_2O	2.70
	Glu260 $O^{\epsilon 2}$	2.71
O4	Arg87 $N^{\eta 2}$	2.77
	Asp131 $O^{\delta 1}$	2.71
O6	H_2O	2.72
O7	H_2O	2.66
	H_2O	3.17
O8	Asp259 $O^{\delta 1}$	2.66
O9	H_2O	2.86
	Asp259 $O^{\delta 2}$	2.53
O10	H_2O	2.74
N5	Asp131 $O^{\delta 2}$	2.76

two very significant changes to the active site. The first is the creation of a large cavity in which the O2 atom of β-Neu5Ac and four water molecules are seen forming hydrogen bond interactions with each other and with protein residues (Table 4). The second is the movement of the side chain of Asn310 to make a strong hydrogen bond to one of these waters at a distance of 2.70 Å. Figures 3 and 4 illustrate the hole created by the Y370G mutation and the hydrogen bonding interactions in this area of the active site, respectively.

DISCUSSION

In 2003, Watson et al. (*10*) reported that three mutants with the strictly conserved tyrosine residue in the sialidase from *M. viridifaciens* replaced are catalytically active inverting sialidases. On the basis of the results for the Y370D mutant, which included a pH−rate profile, a product study, and the effect of leaving group ability on the catalytic rate constants, Watson et al. (*10*) concluded that the Y370D mutant likely operates via a dissociative mechanism. Furthermore, these authors concluded that removal of the strictly conserved tyrosine residue, the catalytic nucleophile, resulted in the generation of a hole in which water could bind and then act as a nucleophile during the catalytic cycle.

To probe in more detail whether such catalytically active inverting mutant sialidases operate via an associative or dissociative mechanism, kinetic studies were performed using the Y370G mutant and sialoside substrates that possess two different leaving group chemistries. That is, kinetics were measured using 4-nitrophenyl sialoside and a sialosyl pyridinium substrate (PNP-αNeu5Ac and DHP-αNeu5Ac, respectively). The difference between these two classes of sialosides is that the enzyme-catalyzed hydrolysis of the pyridinium substrate (**3**) can be accelerated by nucleophilic catalysis, but not by acid catalysis, whereas hydrolysis of the aryl substrate (**1a**) can, in principle, be expedited by both types of catalysis.

The catalytic proficiencies (CPs) listed in Table 3 show that mutation of the general acid catalyst (D92G mutant) actually increases the CP value for hydrolysis of **3**, while the CP value for hydrolysis of **1a** is decreased slightly. These observations are consistent with the notion that acid catalysis is either unimportant (PNP-αNeu5Ac) or impossible (DHP-αNeu5Ac) during hydrolysis of these non-natural substrates. In contrast, removal of the nucleophilic tyrosine residue (Y370G mutant) results in a catastrophic loss of catalytic activity for hydrolysis of the substrate in which acid catalysis is impossible (**3**), yet efficient hydrolysis of **1a** still occurs with the Y370G mutant enzyme. Given that DANA is neither a product nor an intermediate in these reactions, it can be inferred that hydrolysis proceeds via a direct substitution mechanism (S_N1 or S_N2).

Consistent with the observations noted above is the conclusion that the wild-type and Y370G mutant enzymes catalyze reaction via S_N2 and S_N1 mechanisms, respectively. In other words, wild-type enzyme-catalyzed cleavage of the glycosidic C−N bond in **3**, a compound in which acid catalysis is prohibited, is greatly accelerated by the correct alignment of a suitable nucleophile that is actively participating in the cleavage reaction, i.e., an associative S_N2-type mechanism, whereas in the case of the Y370G inverting mutant, the nucleophilic water does not assist in departure of the pyridine leaving group even though the conserved glutamic acid residue (E260), which in the wild-type enzyme presumably acts as a general base catalyst, is still correctly positioned. In other words, the Y370G mutant-catalyzed reaction involves a dissociative S_N1-type mechanism; that is, nucleophilic attack is not coupled to aglycon departure. Clearly, during hydrolysis of aryl sialosides, acid catalysis is a more important contributor to the observed rate acceleration (CP) for the Y370G mutant than it is for the wild-type enzyme.

This strong kinetic evidence that the wild-type *M. viridifaciens* sialidase operates via a mechanism in which nucleophilic attack is concerted with leaving group departure is in

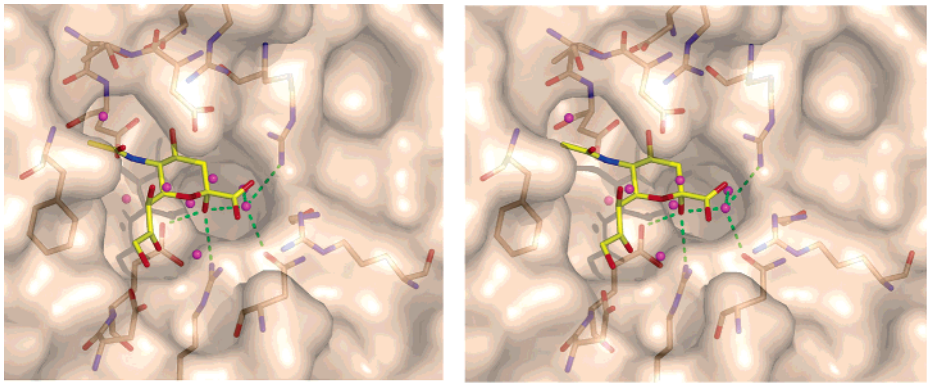

FIGURE 3: Stereoview of the active site of the MvNA Y370G mutant. The view is looking down onto the ligand, β-Neu5Ac, colored yellow. The molecular surface is shown in half-transparency. The hole generated by the mutation can be seen directly beneath the O2 atom of the ligand. The water molecules are shown as magenta colored spheres, with selected hydrogen bonds as dashed green lines.

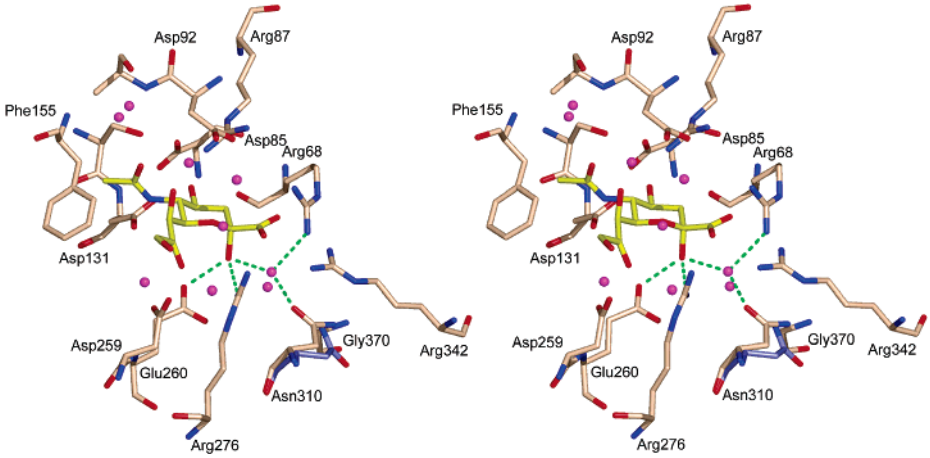

FIGURE 4: Stereoview of the active site of the MvNA Y370G mutant. The mutant active site is colored wheat, and the position of Asn310 in the wild-type structure (PDB entry 1EUS) is colored slate. The selected hydrogen bonds to the O2 atom of the ligand, β-Neu5Ac, are shown as dashed green lines. Four water molecules (magenta) can be seen sitting in the hole generated by the absence of Tyr370. The movement of Asn310 in the mutant structure can also clearly be seen to make a new hydrogen bond to one of these water molecules.

agreement with the conclusion made by Yang et al. (*31*), based on anomeric ^{13}C kinetic isotope effects, that the mechanism used by the *trans*-sialidase from *T. cruzi* is S_N2 in nature.

The conclusion that the Y370G mutant operates via an S_N1 mechanism in which C−O bond cleavage is rate-determining is further strengthened by an analysis of the effect of leaving group ability on the kinetic rate parameters. The β_{lg} value for the S_N1-like uncatalyzed spontaneous hydrolysis of aryl sialosides is −1.22 (*32*), a value that is only slightly larger than those calculated for the Y370G mutant-catalyzed reactions (Figure 1). It can therefore be concluded that the bound water molecule can only weakly assist leaving group departure, at best. Of note, the Y370G mutant possesses kinetic parameters for the hydrolysis of 3′-sialyllactose (**2**) that are within 1 order of magnitude of those reported for the Y370D mutant (*10*). Therefore, it can be concluded that the Y370D mutant also reacts via a dissociative (S_N1-like) mechanism.

Of note, the *M. viridifaciens* sialidase efficiently processes a broad range of substrate structures. Specifically, the CP for the hydrolysis of **3** (Table 3) is between 60- and 1200-fold greater than those reported for the enzyme-catalyzed hydrolysis of pyridinium α-D-*N*-acetylneuraminide by a series of bacterial and viral sialidases (*33*).

The structure of the Y370G complex with the first-formed product of the enzymatic reaction, i.e., β-NeuAc, neatly demonstrates the source of the attacking water from the hole generated by the absence of the phenol ring of Tyr370 (Figure 3). Furthermore, analysis of the hydrogen bond interactions (Table 4), which shows the conserved active site general base (Glu260) to be only 2.71 Å from O2 and 2.7 Å from one of these water molecules, raises the possibility that strong H-bonding to this residue maintains a sufficient distance between the critical water molecule and the anomeric center to prevent nucleophilic attack until after formation of the oxacarbenium ion (S_N1). In other words, nucleophilic attack is delayed until the growing cation−lone pair interaction between the nascent cationic center and the water molecule overcomes the H-bonding to the glutamate residue, whereas in the wild-type MvNA, the nucleophilic oxygen atom (Tyr370) is held in an optimal position such that nucleophilic attack occurs prior to the complete buildup of positive charge on the anomeric center (S_N2).

CONCLUSIONS

In summary, kinetic studies are consistent with the conclusion that the wild-type sialidase from *M. viridifaciens* catalyzes hydrolysis with a direct nucleophilic attack of the active site tyrosine residue at the anomeric center, whereas

the nucleophilic mutant (Y370G) operates via a dissociative mechanism in which a bound water molecule attacks the nascent oxacarbenium ion center after leaving group departure to give β-NeuAc as the first-formed product. The three-dimensional structure of the Y370G mutant shows that removal of the nucleophilic tyrosine residue generates a hole in which water is bound and that minor modifications to the surrounding residues occur to facilitate hydrogen bonding to these water molecules.

ACKNOWLEDGMENT

We thank Dr. Arun Narine for synthesizing DANA.

REFERENCES

1. Saito, M., and Yu, R. K. (1995) in *Biology of the Sialic Acids* (Rosenberg, A., Ed.) pp 261−313, Plenum Press, New York.
2. Corfield, T. (1992) Bacterial sialidases: Roles in pathogenicity and nutrition, *Glycobiology 2*, 509−521.
3. Taylor, G. (1996) Sialidases: Structures, biological significance and therapeutic potential, *Curr. Opin. Struct. Biol. 6*, 830−837.
4. Vimr, E. R. (1994) Microbial sialidases: Does bigger always mean better? *Trends Microbiol. 2*, 271−277.
5. Chong, A. K. J., Pegg, M. S., Taylor, N. R., and Von Itzstein, M. (1992) Evidence for a sialosyl cation transition-state complex in the reactivity of sialidase from influenza virus, *Eur. J. Biochem. 207*, 335−343.
6. Wilson, J. C., Angus, D. I., and Von Itzstein, M. (1995) ^{1}H NMR evidence that *Salmonella typhimurium* sialidase hydrolyzes sialosides with overall retention of configuration, *J. Am. Chem. Soc. 117*, 4214−4217.
7. Davies, G., Sinnott, M. L., and Withers, S. G. (1998) in *Comprehensive Biological Catalysis* (Sinnott, M. L., Ed.) pp 119−209, Academic Press, San Diego.
8. Watts, A. G., Damager, I., Amaya, M. L., Buschiazzo, A., Alzari, P., Frasch, A. C., and Withers, S. G. (2003) *Trypanosoma cruzi trans*-sialidase operates through a covalent sialyl-enzyme intermediate: Tyrosine is the catalytic nucleophile, *J. Am. Chem. Soc. 125*, 7532−7533.
9. Amaya, M. F., Watts, A. G., Damager, T., Wehenkel, A., Nguyen, T., Buschiazzo, A., Paris, G., Frasch, A. C., Withers, S. G., and Alzari, P. M. (2004) Structural insights into the catalytic mechanism of *Trypanosoma cruzi trans*-sialidase, *Structure 12*, 775−784.
10. Watson, J. N., Dookhun, V., Borgford, T. J., and Bennet, A. J. (2003) Mutagenesis of the conserved active-site tyrosine changes a retaining sialidase into an inverting sialidase, *Biochemistry 42*, 12682−12690.
11. Varghese, J. N., and Colman, P. M. (1991) Three-dimensional structure of the neuraminidase of influenza virus A/Tokyo/3/67 at 2.2 Å resolution, *J. Mol. Biol. 221*, 473−486.
12. Guo, X., Laver, W. G., Vimr, E., and Sinnott, M. L. (1994) Catalysis by two sialidases with the same protein fold but different stereochemical courses: A mechanistic comparison of the enzymes from influenza A virus and *Salmonella typhimurium*, *J. Am. Chem. Soc. 116*, 5572−5578.
13. Barnes, J. A., and Williams, I. H. (1996) Quantum mechanical/molecular mechanical approaches to transition state structure: Mechanism of sialidase action, *Biochem. Soc. Trans. 24*, 263−268.
14. Watson, J. N., Newstead, S., Dookhun, V., Taylor, G., and Bennet, A. J. (2004) Contribution of the active site aspartic acid to catalysis in the bacterial neuraminidase from *Micromonospora viridifaciens*, *FEBS Lett. 577*, 265−269.
15. Wang, Q. P., Graham, R. W., Trimbur, D., Warren, R. A. J., and Withers, S. G. (1994) Changing enzymatic-reaction mechanisms by mutagenesis: Conversion of a retaining glucosidase to an inverting enzyme, *J. Am. Chem. Soc. 116*, 11594−11595.
16. Moracci, M., Trincone, A., Perugino, G., Ciaramella, M., and Rossi, M. (1998) Restoration of the activity of active-site mutants of the hyperthermophilic β-glycosidase from *Sulfolobus solfataricus*: Dependence of the mechanism on the action of external nucleophiles, *Biochemistry 37*, 17262−17270.
17. Viladot, J. L., Canals, F., Batllori, X., and Planas, A. (2001) Long-lived glycosyl-enzyme intermediate mimic produced by formate re-activation of a mutant endoglucanase lacking its catalytic nucleophile, *Biochem. J. 355*, 79−86.
18. Shallom, D., Belakhov, V., Solomon, D., Shoham, G., Baasov, T., and Shoham, Y. (2002) Detailed kinetic analysis and identification of the nucleophile in α-L-arabinofuranosidase from *Geobacillus stearothermophilus* T-6, a family 51 glycoside hydrolase, *J. Biol. Chem. 277*, 43667−43673.
19. Cobucci-Ponzano, B., Trincone, A., Giordano, A., Rossi, M., and Moracci, M. (2003) Identification of the catalytic nucleophile of the family 29 α-L-fucosidase from *Sulfolobus solfataricus* via chemical rescue of an inactive mutant, *Biochemistry 42*, 9525−9531.
20. Knoll, T. L., and Bennet, A. J. (2004) Aqueous methanolysis of an α-D-*N*-acetylneuraminyl pyridinium zwitterion: Solvolysis occurs with no intramolecular participation of the anomeric carboxylate group, *J. Phys. Org. Chem. 17*, 478−482.
21. Baggett, N., and Marsden, B. J. (1982) Reinvestigation of the synthesis of 4-methylcoumarin-7-yl 5-acetamido-3,5-dideoxy-α-D-*glycero*-D-*galacto*-2-nonulopyranosidonic acid, a fluorogenic substrate for neuraminidase, *Carbohydr. Res. 110*, 11−18.
22. Petrie, C. R., Sharma, M., Simmons, O. D., and Korytnyk, W. (1989) Synthesis of analogs of *N*-acetylneuraminic acid and their effect on CMP-sialate synthase, *Carbohydr. Res. 186*, 326−334.
23. Leslie, A. G. W. (1992) Recent changes to the MOSFLM package for processing film and image plate data, *Joint CCP4 & ESF-EAMCB Newsletter on Protein Crystallography*, No. 26, Daresbury Laboratory, Warrington, U.K.
24. Evans, P. R. (1997) SCALA, *Joint CCP4 & ESF-EAMCB Newsletter on Protein Crystallography*, No. 33, pp 22−24, Daresbury Laboratory, Warrington, U.K.
25. Collaborative Computational Project No. 4 (1994) The CCP4 suite: Programs for Protein Crystallography, Number 4, *Acta Crystallogr. D50*, 760−763.
26. Navaza, J. (1994) AMoRe: An automated package for molecular replacement, *Acta Crystallogr. A50*, 157−163.
27. Murshudov, G. N. (1997) Refinement of macromolecular structures by the maximum-likelihood method, *Acta Crystallogr. D53*, 240−255.
28. Jones, T. A., Bergdoll, M., and Kjeldgaard, M. (1990) in *Crystallographic and Modeling Methods in Molecular Design* (Ealick, S., Ed.) pp 189−195, Springer-Verlag, Berlin.
29. Perrakis, A., Morris, R., and Lamzin, V. S. (1999) Automated protein model building combined with iterative structure refinement, *Nat. Struct. Biol. 6*, 458−463.
30. Gaskell, A., Crennell, S., and Taylor, G. (1995) The three domains of a bacterial sialidase: A β-propeller, an immunoglobulin module and a galactose-binding jellyroll, *Structure 3*, 1197−1205.
31. Yang, J., Schenkman, S., and Horenstein, B. A. (2000) Primary ^{13}C and β-secondary ^{2}H KIEs for *trans*-sialidase. A snapshot of nucleophilic participation during catalysis, *Biochemistry 39*, 5902−5910.
32. Ashwell, M., Guo, X., and Sinnott, M. L. (1992) Pathways for the hydrolysis of glycosides of *N*-acetylneuraminic acid, *J. Am. Chem. Soc. 114*, 10158−10166.
33. Watson, J. N., Knoll, T. L., Chen, J. H., Chou, D. T. H., Borgford, T. J., and Bennet, A. J. (2005) Use of conformationally restricted pyridinium α-D-*N*-acetylneuraminides to probe specificity in bacterial and viral sialidases, *Biochem. Cell Biol. 83*, 115−122.
34. Cruickshank, D. W. (1999) Remarks about protein structure precision, *Acta Crystallogr. D55*, 583−601.
35. Schneider, T. R. (2002) A genetic algorithm for the identification of conformationally invariant regions in protein molecules, *Acta Crystallogr. D58*, 195−208.
36. Serjeant, E. P., and Dempsey, B. (1979) *Ionisation constants of organic acids in aqueous solution*, Pergamon Press, New York.
37. Segel, I. H. (1975) *Enzyme kinetics: Behavior and analysis of rapid equilibrium and steady state enzyme systems*, Wiley, New York.
38. Dookhun, V., and Bennet, A. J. (2005) Unexpected stability of aryl β-*N*-acetylneuraminides in neutral solution: Biological implications for sialyl transfer reactions, *J. Am. Chem. Soc. 127*, 7458−7465.

BI050517T